DYNAMIC COMPLIANCE OF SHALLOW FOOTINGS ON NONLINEAR SOIL

M J PENDER[1]

SUMMARY

The features of a model for the cyclic stress-strain behaviour of cohesive soil are explained and the application of the model to estimating the dynamic compliance of footings under vertical cyclic loading is illustrated. The dynamic calculations were done with the *FLAC* (Fast Lagrangian Analysis of Continua) software. The model is formulated within the framework of critical state soil mechanics. However, unlike the classical critical state models, Cam clay and modified Cam clay, this model has inelastic behaviour for overconsolidated soil. The particular version of the model implemented herein is for a lightly overconsolidated soil, which deforms in an undrained manner at constant mean principal effective stress. With the addition of small-strain elastic shear behaviour the model is shown to represent well the degradation, with shear strain amplitude, in the apparent shear modulus and equivalent viscous damping ratio. The calculations herein indicate that there are two distinct aspects of shallow foundation response to cyclic loading – cyclic deformation and the accumulation of permanent settlement; the permanent settlement was found to be the more significant of the two. It was also noted that the dynamic compliance of the foundation on nonlinear soil exhibited greater variation with cyclic loading frequency than the same foundation on an elastic soil.

INTRODUCTION

The purpose of this paper is to demonstrate the application of a constitutive relationship for the cyclic loading of lightly overconsolidated soil to predicting the dynamic compliance of statically loaded shallow foundations. The model [Pender, 1977a, 1977b and 1978] is formulated within the framework of critical state soil mechanics but, unlike the classical critical state models, Cam clay and modified Cam clay, it postulates the occurrence of plastic deformation whenever there is a change in shear stress. Because of this, realistic modelling of cyclic behaviour is possible. With the addition of the small-strain elastic shear modulus, the soil parameters needed are those for the Cam clay models, usually obtained from standard soil testing.

In general the equations for incremental strain and stress changes cannot be expressed in closed form, so numerical integration is necessary. However, for one special case, the shear strains can be expressed in closed form. This is when the mean principal effective stress is constant at p_{cs}, the value on the critical state line corresponding to the current void ratio of the soil. An earlier publication [Pender 1977a] showed how this version of the model generates the well-known variations, with cyclic shear strain amplitude, of apparent shear modulus and equivalent viscous damping ratio.

The numerical calculations of the response of a strip foundation discussed in this paper were done using the *FLAC* (Fast Lagrangian Analysis of Continua) software [Itasca, 1998]. *FLAC* provides a facility for incorporation of user defined constitutive models. The performance of the author's model when incorporated into *FLAC* has been investigated [Pender, 1999]. The calculations herein indicate that there are two distinct aspects of shallow foundation response to cyclic loading – cyclic deformation and the accumulation of permanent settlement. The permanent settlement was found to be the more significant of the two. It was also

[1] *Department of Civil and Resource Engineering, University of Auckland, New Zealand. Email: m.pender@auckland.ac.nz*

noted that the dynamic compliance of the foundation on nonlinear soil exhibited greater variation with cyclic loading frequency than the same foundation on an elastic soil.

2. BACKGROUND AND DESCRIPTION OF THE MODEL

The model is formulated within the framework of work hardening plasticity but, as it is assumed that plastic strains occur for all changes in shear stress, the yield surface is carried along with the stress point. This makes for simple computations, as it is not necessary to check for yielding at each step. In addition at small strains the elastic stiffness of the soil is important, so the shear strain is the sum of elastic and plastic parts. The detailed derivation of the equations of the model is given elsewhere [Pender 1977b, 1978].

The stress and strain variables used in the model are: q = 3/√2 (octahedral shear stress), p = mean principal effective stress, η = the ratio q/p, and ε = 1/√2 (octahedral shear strain); in some contexts the engineering shear strain, γ, is also used. The model discussed here is for the special case when $p = p_{cs}$, for which there is no volume change and thus undrained deformation. The closed form equation for the plastic distortion is given by:

$$\varepsilon^{p}_{p_o=p_{cs}} = \frac{2\kappa}{\mathrm{M}^2(1+e)}\left\{(A\mathrm{M}-\eta_0)\ln\left(\frac{A\mathrm{M}-\eta_o}{A\mathrm{M}-\eta}\right)-(\eta-\eta_o)\right\}+\varepsilon^{p}_{o} \qquad (1)$$

where:

where:	A	+1 for compression and –1 for extension
	M	critical state friction parameter
	κ	- slope of the swelling line in the e *ln*p plane
	e	void ratio
	p_{cs}	p on the critical state line corresponding to e
	η_o	value of η at the last turning point
	ε^{p}_{o}	accumulated distortion at the last turning point.

Cyclic loading is controlled by the *A* parameter and the value of η_o. The parameter *A* indicates the direction of the loading, that is whether the soil is being deformed in compression or extension. Each time there is a change in direction of the loading, that is the commencement of a new half cycle, the values for *A* and η_o (or q_o if equations 4 or 5 are in use) are reset. Stress-strain loops for cyclic loading between fixed shear stresses are shown in the left-hand plot in Figure 1 and between fixed strain limits in the right-hand plot.

The above equation, with the addition of small strain elastic distortion, can be used to give the apparent shear modulus, G, and equivalent viscous damping ratio, D, both of which are defined in Figure 2, for steady state cycling between fixed values of the stress ratio, η_j. The expression for the apparent shear modulus is:

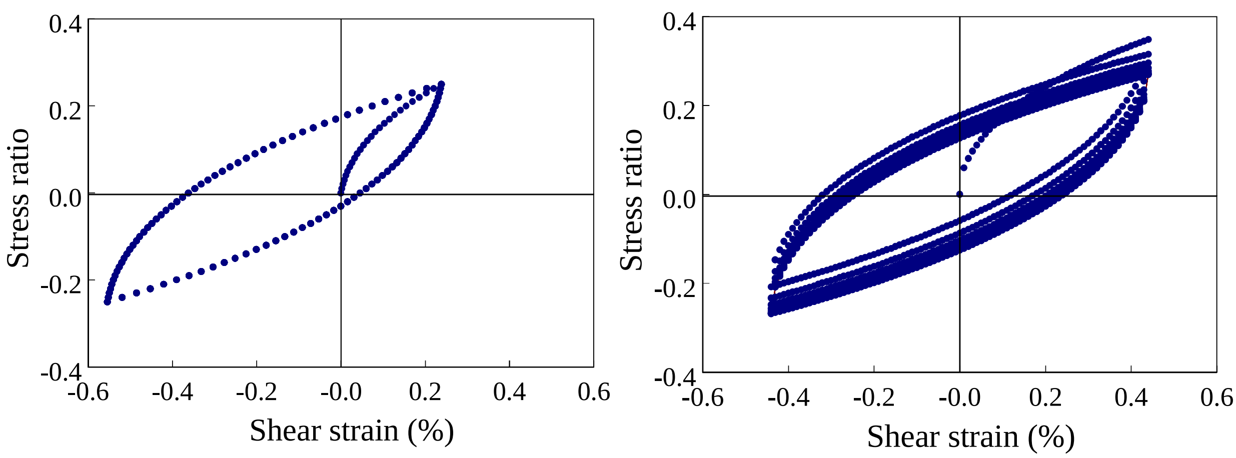

Figure 1: Cyclic stress-strain response calculated with equation 1. Left: cycling between fixed stress limits, right: cycling between fixed strain limits.

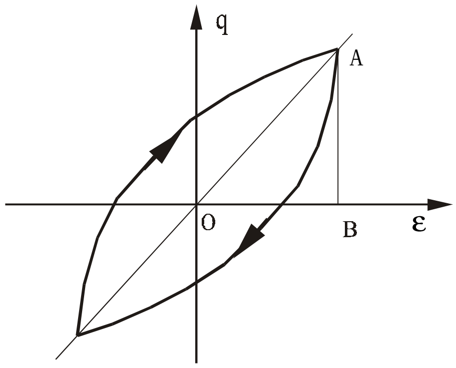

G = slope(OA) / 3

D = area of loop / 4π area (ΔOAB)

Figure 2: Definitions of apparent shear modulus and equivalent viscous damping ratio.

$$\frac{G}{s_u} = \frac{2\eta_j(1+e)}{3\kappa\left\{\left(1+\frac{\eta_j}{\mathrm{M}}\right)\ln\left(\frac{\mathrm{M}+\eta_j}{\mathrm{M}-\eta_j}\right)-\frac{2\eta_j}{\mathrm{M}}\right\}+\frac{\mathrm{M}p_{cs}\eta_j(1+e)}{G_e}} \tag{2}$$

where: G_e is the small strain elastic shear modulus of the soil
s_u is the undrained shear strength of the soil.

The above equation, and equation (3), correct a previous error [Pender, 1977a], wherein it was assumed that the secant modulus between the end points of a q - ε loop is the shear modulus G, in fact it is 3G.

The equivalent viscous damping ratio is given by:

$$D = \frac{\left(\frac{2}{\pi}\right)\left(1+\frac{\eta_j}{\mathrm{M}}\right)\left\{\ln\left(\frac{\mathrm{M}+\eta_j}{\mathrm{M}-\eta_j}\right)-\frac{2\eta_j}{\mathrm{M}}\right\}}{\left(\frac{\eta_j}{\mathrm{M}}\right)\left\{\left(1+\frac{\eta_j}{\mathrm{M}}\right)\ln\left(\frac{\mathrm{M}+\eta_j}{\mathrm{M}-\eta_j}\right)-\frac{2\eta_j}{\mathrm{M}}\right\}+\frac{\eta_j^2 p_{cs}(1+e)}{3\kappa G_e}} \tag{3}$$

Figure 3 shows that equations (2) and (3) give a good representation of actual G and D - γ curves.

3. IMPLEMENTATION OF THE MODEL IN *FLAC*

3.1 The tangent modulus approach

In principle, the model should be formulated in terms of work-hardening plasticity. However, as there are no volumetric strains for the $p = p_{cs}$ condition, an attractive initial step is to use a pseudo-elastic approach in which the tangent shear modulus is a function of the current stresses; that is indeed what is done here. The provision of the simple hyperbolic constitutive model, HYP.FIS, in the library of FISH functions for *FLAC* version 3.4, was a particularly helpful starting point for developing the *FLAC* version of the author’s model; the main extension from HYP.FIS was the handling of cyclic loading.

As *FLAC* supplies the user defined constitutive model with strain increments an incremental form of equation (1) is needed. This is:

$$d\varepsilon^p = \frac{2\kappa}{p_{cs}\mathrm{M}^2(1+e)}\frac{(q-q_o)dq}{(A\mathrm{M}p_{cs}-q)} \tag{4}$$

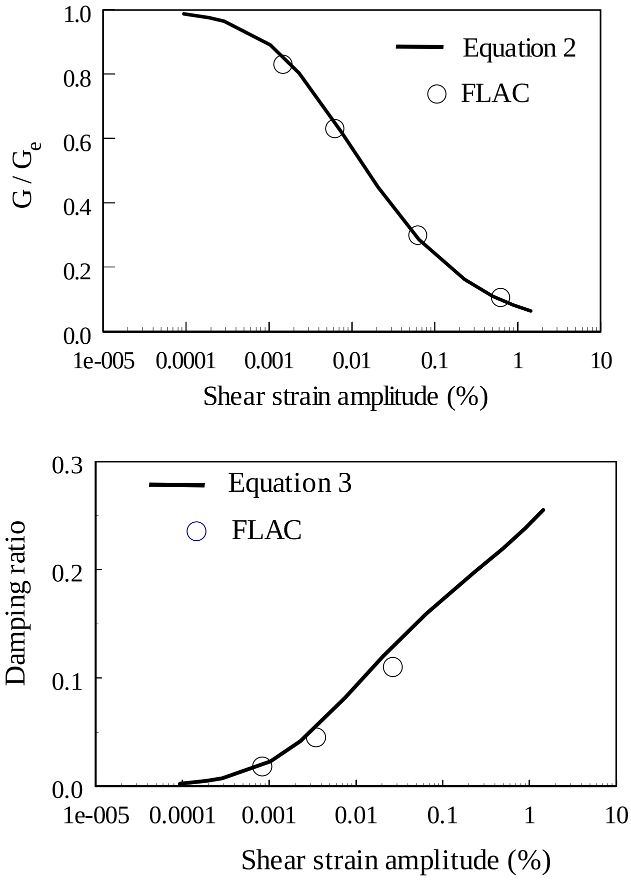

Figure 3: Comparison between the apparent shear modulus (upper) and equivalent viscous damping ratio (lower) calculated with equations (2) and (3) and with the *FLAC* implementation of the model.

where: q_o is the value of q at the last turning point.

From this the tangent shear modulus for plastic distortion is obtained

$$G_p = \frac{p_{cs} \mathrm{M}^2 (1+e)}{6\kappa} \frac{(A\mathrm{M} p_{cs} - q)}{(q - q_o)} \tag{5}$$

The equivalent tangent modulus, including both elastic and plastic contributions, is:

$$G_{\text{tangent}} = \frac{G_e G_p}{G_e + G_p} \tag{6}$$

FLAC requires a bulk modulus (K) as well as a maximum value for the shear modulus (G_e) of the soil. Although the tangent shear modulus varies with stress it is assumed in the *FLAC* implementation of the model that the bulk modulus is constant; this is appropriate, as the mean principal effective stress remains at p_{cs} in the special case of the model considered in this paper. Further details of the *FLAC* implementation and examples are given by Pender (1999).

3.2 Apparent shear modulus and equivalent viscous damping ratio

In Figure 3 the values of the apparent shear modulus and equivalent viscous damping ratio against strain amplitude obtained with equations (2) and (3) are compared with those obtained using the *FLAC* implementation of the model. The open circles in Figure 3 were obtained from analysis of the free vibration response of a single zone calculated with *FLAC* following gravity turn-on loading, further details are given in Pender (1999). Note that these calculations were done with no *FLAC* damping, that is neither Rayleigh nor local damping was set, thus the damping evident in the lower part of Figure 3 is entirely a consequence of the hysteretic damping implicit in the soil model. Calculations were done for a range of values of the vertical acceleration from 0.05 to

0.8 g, so generating a range of shear strain amplitudes. The calculated damping values, averages for the first four and a half cycles of vibration, are compared in the lower part of Figure 3 with the values given by equation (3). It is apparent that the free vibration damping values tend to be marginally less than those given by equation (3). The explanation is that equations (2) and (3) apply to closed stress-strain loops, such as those in the plots in Figure 1. In the free vibration data plotted in Figure 5 significant damping occurs in the first few half cycles, evidently this is slightly less than the damping given by equation (3) as the stress-strain loops are not closed.

The calculations on which Figures 1 and 3 are based used the following soil parameters: e 1.0, M 1.0, κ 0.01, p_{cs} 100 kPa (thus the undrained shear strength = $\frac{1}{2}Mp_{cs}$ = 50 kPa), density 1.8 tonne/m^3, G_e 20 MPa, and K 60 MPa. The ratio of the small strain shear modulus to the undrained shear strength obtained from these input values is about 400, which is consistent with values of this ratio which have been found for overconsolidated soil [Weiler, 1988].

4. VERTICAL VIBRATION OF A SHALLOW FOOTING ON A NONLINEAR SOIL DEPOSIT

4.1 *FLAC* calculations for two-dimensional deformation

FLAC returns strain increments to the user defined constitutive relationship, thus the criterion for changes in loading direction depends on the current strain increments relative the cumulative strain since the last turning point. In the earlier implementation of the author's model in *FLAC*, [Pender, 1999], all the calculations were for one-dimensional cyclic loading. In these situations changes in loading direction are obvious, but this is not so for two-dimensional loading. In the calculations herein the procedure suggested by Cundall (1998), when implementing in *FLAC* the Martin et al (1975) pore pressure generation model for saturated sand, is followed. This suggests that the turning point criterion be based on the dot product of the current strain increment vector with the cumulative strain vector since the last turning point. When the dot product changes sign the strain vector has passed through a maximum and hence a reversal in the loading direction has occurred. At this point the values of q_o and *A* in equation (5) are reset and $G_{tangent}$ becomes equal to G_e.

4.2 Details of the *FLAC* modelling for the footing

The calculations reported below are for the dynamic response of a strip footing (2D plane strain) on the surface of a soil layer. The footing was modelled as rigid using a special feature of *FLAC*, which enables grid point displacements to be slaved together. This makes it possible to model rigid footing behaviour without the need to add very stiff zones to represent the footing and so incur a severe time penalty in the calculation process as a large contrast in moduli requires that the numerical time step be reduced. The footing was subject to 10 cycles of sinusoidal pressure loading. The details of the footing, finite difference mesh, and dynamic boundary conditions are shown in Figure 4. Because of symmetry only half the 5 m wide footing is modelled.

Soil properties:

Shear wave velocity	150m/sec
Small stain shear modulus	40MPa
Bulk modulus	200MPa
Void ratio	1.0

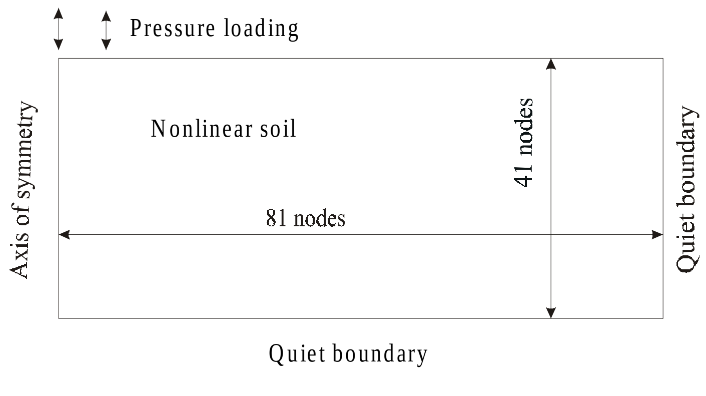

Figure 4: Details of the dynamically loaded shallow strip footing on nonlinear soil.

The soil layer had a shear wave velocity of 150 m/sec (that is G_e of 40 MPa) and an undrained shear strength of 100 kPa. These properties represent a “good” foundation material for which a shallow foundation would be appropriate. The small strain elastic soil properties are such as to give a Poisson’s ratio of about 0.4.

The quiet boundaries in *FLAC* are less effective at handling Rayleigh waves, so in addition to the hysteretic damping in the model 5% Raleigh damping was applied. This ensured a smooth response for the footing over the 10 cycles of dynamic loading, without this damping reflected waves are likely to mask the foundation behaviour.

Before the dynamic response can be calculated there are two preliminary calculation steps. First the in situ stresses in the ground must be introduced. This is done by having the ground surface free of load and applying gravity to the soil mass. Once these stresses are installed the static loading is applied to the foundation. This is done for static bearing capacity factors of safety of 2, 3 and 4. Only after these two steps have been done can the dynamic loading be applied. The nonlinear stress strain behaviour of the soil means that it is important to have the shear stresses generated by the in situ stresses and the static foundation loading in the ground before the dynamic loading is applied. The bearing capacity factors of safety of 2, 3, and 4 represent a typical design value with a lower and a higher value to evaluate the sensitivity of the results to changes in this parameter.

The amplitude of the cyclic pressure applied to the foundation ranged from very small values up to 86 kPa, which was sufficient to reduce the static factor of safety of 3 down to 2. The standard frequency parameter for characterising footing response is:

$$a_o = \frac{\omega B}{V_s} \tag{7}$$

where: a_o is the dimensionless frequency parameter
ω is the excitation frequency in radians per second
B is the half width of the footing
V_s is the shear wave velocity for the soil.

Footing response calculations were done for a range of values for a_o of 0.5 to 2.5. This corresponds to a frequencies of about 4 Hz to 40 Hz.

4.3 Results

The results of the dynamic response calculations are presented in Figures 5 and 6.

In Figure 5 two sets of results are presented for a_o equal to 1.5. On the left hand side average cyclic displacement amplitude over 10 cycles is compared for elastic and nonlinear soil behaviour. As expected there is no significant difference between the average displacement amplitude for elastic and nonlinear behaviour at low levels of cyclic loading, and as the cyclic pressure amplitude increases the compliance of the foundation on the nonlinear soil becomes greater than that on the linear elastic material. On the right-hand side of Figure 5 the footing response for three values of the factor of safety are plotted when the cyclic pressure amplitude is 86 kPa. The plots show that the cyclic amplitude of the motion for the three values of the factor of safety are very similar and that the pattern of the accumulation of permanent deformation is also similar. Some differences are apparent for the permanent deformation in that there seems to be a change in behaviour after at about 0.2 seconds. Up to that time it is seen that the lowest factor of safety has the largest permanent deformation after which there is a steady accumulation of permanent deformation with the footing having the highest static factor of safety being seen to increase more than the others. Perhaps more important though, is the observation that the accumulation of permanent deformation is more significant than the cyclic amplitude, so that at the completion of the cyclic loading permanent deformation is the most striking effect.

In Figure 6 results are presented for cyclic loading from a static factor of safety of 4 and a cyclic pressure amplitude of 86 kPa over the range of frequencies investigated. On the left hand side the normalised mean displacement amplitudes are presented both for elastic and nonlinear soil behaviour. The amplitude at a_o equal to 2.5 is used to normalise the other amplitudes. The curve for elastic behaviour follows the well known results that the vertical compliance of a footing increases as the frequency decreases. (It is shown in the *FLAC* manual that for elastic soil the numerical solution for this case corresponds to the solution obtained by other methods.) It is apparent that this frequency effect is even more significant when the soil behaviour is nonlinear. On the right hand side the mean amplitude of the cyclic response is again contrasted with the accumulation of permanent

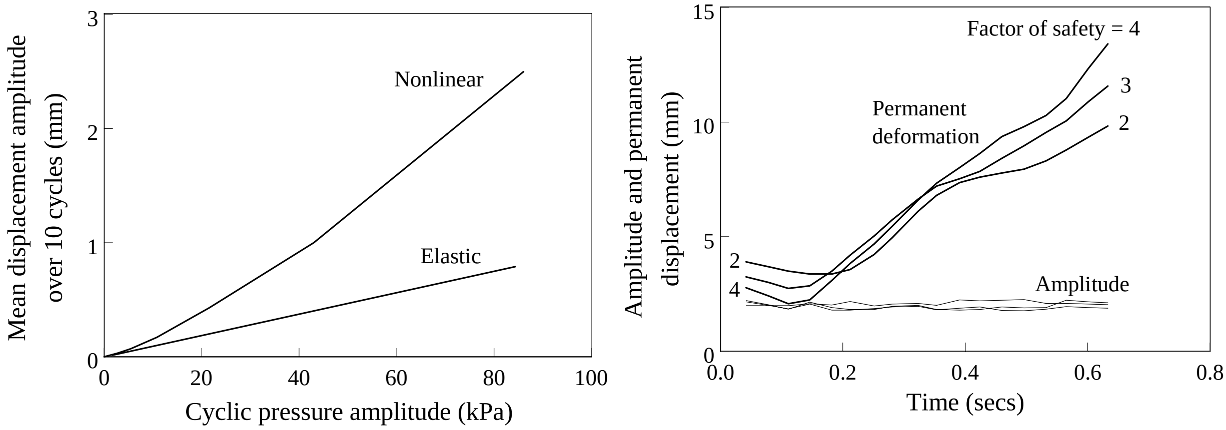

Figure 5: Left-hand side: elastic and nonlinear mean displacement amplitudes. Right-hand side: effect of factor of safety when the cyclic pressure amplitude is 86 kPa. (a_o for both diagrams 1.5.)

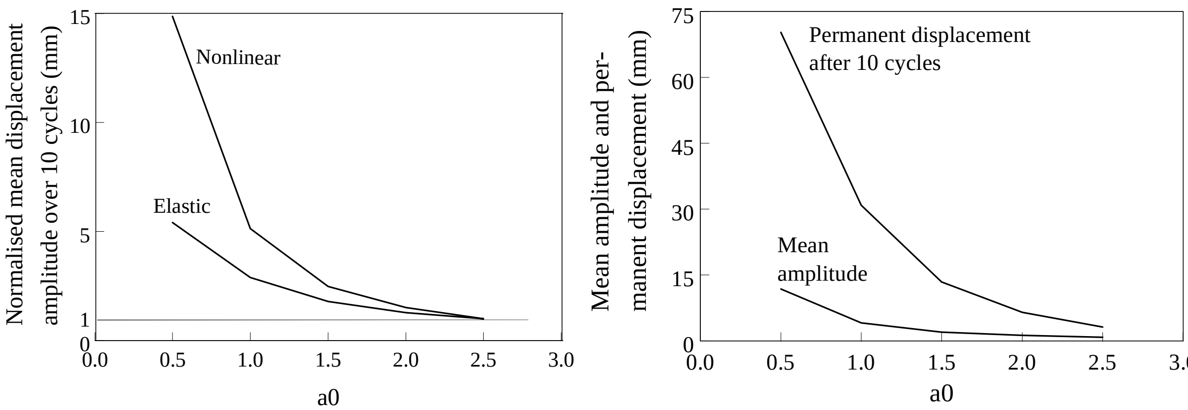

Figure 6: Left-hand side: elastic and nonlinear mean settlement amplitudes as a function of the frequency parameter. Right-hand side: comparison of mean settlement amplitude and the accumulated permanent settlement after 10 cycles. (For both diagrams the factor of safety is 4 and the cyclic pressure amplitude is 86 kPa.) and the cyclic pressure amplitude is 86 kPa.)

displacement after 10 cycles. This confirms the tend in Figure 5 and shows that the accumulation of permanent deformation is the most striking aspect of the footing behaviour over the full frequency range.

5. DISCUSSION AND EVALUATION

Surprising, at first sight, is the observation from the results that the accumulation of permanent settlement is so much more significant than the cyclic settlement amplitude. This may reflect the effect of static loading on the foundation prior to the cyclic excitation. As part of the undrained shear strength of the soil is mobilised by the static loading there is a shear stress bias in each zone during the cyclic loading. This bias means that during the cyclic loading the shear stress cycle for a particular zone is unlikely to be symmetrical about the zero shear stress axis and, in fact, there may not even be a reversal of shear stress and with each cycle. Thus a cyclic increase in shear strain will occur which is manifested in the footing response calculations with the cycle by cycle accumulation of settlement

Also surprising was the observation that the footing settlement is not greatly affected by the static factor of safety. One might have thought that the footing with the factor of safety of 2 would have a greater cyclic settlement amplitude and accumulate permanent settlement at a greater rate than the footings with the larger factors of safety.

Clearly the next step in the development of this work is to calculate the earthquake dynamic soil structure interaction of a structure with discrete foundations on each side. In this situation the rocking response of the structure is transmitted to the underlying soil through vertical up and down motions of the foundations in the manner calculated above.

6. CONCLUSIONS

The vertical dynamic response of a strip foundation on a nonlinear soil has been calculated. A soil model that represents well the variation with shear strain of apparent shear modulus and equivalent viscous damping ratio was implemented in the *FLAC* software, which has the facility for calculating dynamic response. The following conclusions were reached:

- It is well known that the dynamic vertical compliance of a strip foundation on an elastic soil varies with the frequency of excitation. It was found that for the strip foundation on nonlinear soil the variation with frequency was more marked than for the foundation on an elastic soil. This is shown in the left-hand side of Figure 6.

- The calculations indicated that there are two distinct aspects of the response to cyclic loading of a shallow foundation on a nonlinear soil – cyclic deformation and the accumulation of permanent settlement. The permanent settlement was found to be the more significant of the two. This is shown in right-hand sides of Figures 5 and 6.

- Calculations were done for the foundation under three initial conditions - static bearing capacity factors of safety of 2, 3 and 4. The right-hand side of Figure 6 shows that the amplitude of the cyclic response was about the same for all three factors of safety. It is also apparent from the same figure that the accumulation of permanent settlement is not greatly different for all three factors of safety.

7. REFERENCES

Cundall, P. A. (1998) “Dynamic Analysis”, Section 3 *Optional Features Volume of the FLAC 3.4 Manual*, pp3-40 to 3-44.

Itasca Consulting Group (1998) “*FLAC 3.4 User Manuals*”, Itasca Consulting Group. Minneapolis, Minnesota.

Martin, G. R., Finn W. D. and Seed H. B. (1975) “Fundamentals of liquefaction under cyclic loading”, *J. Geotech. Eng.*, ASCE, 101(GT5), pp423-438.

Pender, M.J. (1977a), “Modelling Soil Behaviour under Cyclic Loading”, *Proc. 9th International Conference of Soil Mechanics and Foundation Engineering, Tokyo,* I, pp325-331.

Pender, M.J. (1977b), “A Unified Model for the Stress-Strain Behaviour of Normally and Overconsolidated Soil”, *Proc. 9th ICSMFE, Tokyo, Specialty Session No.9, Constitutive Relationships for Soils,* pp213-222.

Pender, M.J. (1978), “A Model for the Behaviour of Overconsolidated Soil”, *Geotechnique,* 28, pp1-25.

Pender, M. J. (1999) “Implementing a soil stress-strain model with hysteretic damping in FLAC”, Proc. of the International Symposium FLAC and Numerical Modelling in Geomechanics, edited by Christine Detourney and Roger Hart, Balkema, pp475-482.

Weiler, W. A. (1988), “Small strain shear modulus of clay”, *Proceedings, ASCE Conference on Earthquake Engineering and Soil Dynamics II: Recent Advances in Ground Motion Evaluation,* Geotechnical Special Technical Publication 20, pp331-335.